J|A|C|S
ARTICLES
Published on Web 10/29/2003

Millisecond Kinetics on a Microfluidic Chip Using Nanoliters of Reagents

Helen Song and Rustem F. Ismagilov*

Contribution from the Department of Chemistry, The University of Chicago, 5735 South Ellis Avenue, Chicago, Illinois 60637

Received April 4, 2003; E-mail: r-ismagilov@uchicago.edu.

Abstract: This paper describes a microfluidic chip for performing kinetic measurements with better than millisecond resolution. Rapid kinetic measurements in microfluidic systems are complicated by two problems: mixing is slow and dispersion is large. These problems also complicate biochemical assays performed in microfluidic chips. We have recently shown (Song, H.; Tice, J. D.; Ismagilov, R. F. *Angew. Chem., Int. Ed.* **2003**, *42*, 768−772) how multiphase fluid flow in microchannels can be used to address both problems by transporting the reagents inside aqueous droplets (plugs) surrounded by an immiscible fluid. Here, this droplet-based microfluidic system was used to extract kinetic parameters of an enzymatic reaction. Rapid single-turnover kinetics of ribonuclease A (RNase A) was measured with better than millisecond resolution using sub-microliter volumes of solutions. To obtain the single-turnover rate constant ($k = 1100 \pm 250$ s^{-1}), four new features for this microfluidics platform were demonstrated: (i) rapid on-chip dilution, (ii) multiple time range access, (iii) biocompatibility with RNase A, and (iv) explicit treatment of mixing for improving time resolution of the system. These features are discussed using kinetics of RNase A. From fluorescent images integrated for 2−4 s, each kinetic profile can be obtained using less than 150 nL of solutions of reagents because this system relies on chaotic advection inside moving droplets rather than on turbulence to achieve rapid mixing. Fabrication of these devices in PDMS is straightforward and no specialized equipment, except for a standard microscope with a CCD camera, is needed to run the experiments. This microfluidic platform could serve as an inexpensive and economical complement to stopped-flow methods for a broad range of time-resolved experiments and assays in chemistry and biochemistry.

Introduction

This paper describes a microfluidic platform (Figure 1) for performing kinetic measurements with better than millisecond resolution. Both fast ($k \approx 1000$ s^{-1}) and slow ($k \approx 1$ s^{-1}) kinetics can be measured using this platform. Even for fastest measurements, each kinetic profile can be obtained using less than 150 nL of solutions of reagents because this system of moving droplets[1] relies on chaotic advection,[2] rather than turbulence,[3] to achieve rapid mixing.

We have recently described[1] and characterized[4] a set of physical phenomena in multiphase fluid flow that solve both the mixing and dispersion problems of microfluidics. Fabrication of these microfluidic devices in PDMS was straightforward,[5] and no specialized equipment except for a standard microscope with a CCD camera was needed to run the experiments. This system removed dispersion by localizing reagents inside aqueous droplets (plugs) formed in a stream of a water-immiscible fluorinated carrier fluid. The width and height of plugs were equal to the cross-sectional dimension (∼20−100 μm) of the channels. The length of the plug may be controlled from ∼1 to ∼10 times the width by varying the ratio of the flow rates of aqueous streams and carrier fluid.[4] Smaller plugs used in kinetics may be formed with better than 5% reproducibility.[4] Each plug carried a mixture of two reagents and a stream of buffer, injected into the microfluidic chip by syringe pumps. Rapid (∼2 ms) mixing[1] was achieved by inducing chaotic flow inside droplets moving through the winding part of the channel. Mixing was quantified by measuring the rate of binding of Ca^{2+} and

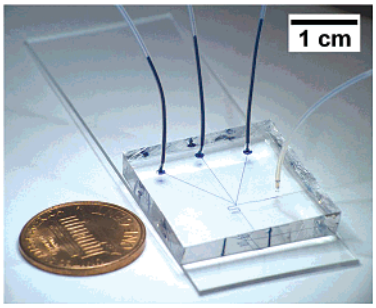

Figure 1. Photograph of a PDMS microfluidic system next to a U.S. penny. The three adjacent Teflon needles were each filled with 2 μL of blue solution, sufficient to measure ∼15 complete kinetic profiles on millisecond scale. The clear Teflon needle was filled with the fluorinated carrier fluid.

(1) Song, H.; Tice, J. D.; Ismagilov, R. F. *Angew. Chem., Int. Ed.* **2003**, *42*, 768−772.
(2) Stroock, A. D.; Dertinger, S. K. W.; Ajdari, A.; Mezic, I.; Stone, H. A.; Whitesides, G. M. *Science* **2002**, *295*, 647−651.
(3) Shastry, M. C. R.; Luck, S. D.; Roder, H. *Biophys. J.* **1998**, *74*, 2714−2721.
(4) Tice, J. D.; Song, H.; Lyon, A. D.; Ismagilov, R. F. *Langmuir* **2003**, *19*, 9127−9133.
(5) McDonald, J. C.; Whitesides, G. M. *Acc. Chem. Res.* **2002**, *35*, 491−499.

Fluo-4. No kinetic parameters could be extracted for this binding reaction.

Here we describe how this microfluidic platform can be used to extract kinetic parameters on millisecond time scale. Four features advance this work beyond our previous report:[1] (i) rapid on-chip dilution, (ii) multiple time range access, (iii) compatibility with an enzyme, and (iv) explicit treatment of mixing for improving time resolution of the system. This paper discusses these points using ribonuclease A (RNase A) kinetics and uses all these features to measure single-turnover kinetics of RNase A with better than millisecond resolution using submicroliter volumes of solutions.

Rapid kinetic measurements are crucial for understanding protein[6] and RNA[7] folding, as well as enzymatic[8−10] and chemical[11] reactivity. These measurements have been possible due to the development of techniques such as stopped-flow[9,10] and quenched-flow.[8] These methods use turbulence to induce rapid mixing of the reagents; they require high (mL/s) flow rates and consume large volumes of samples. These methods are expensive and are not sufficiently frugal for characterization of many biomolecules produced in small quantities by genomics and proteomics efforts.[12]

Microfluidic systems are attractive for performing measurements using minute amounts of reagents. They have been used to characterize kinetics of biochemical[13−15] systems on time scales ranging from minutes[15] to seconds.[13,14] Microfluidic systems have not replaced turbulence-based rapid kinetic instruments because of the two problems that limit the resolution: mixing of reagent streams across the channel is slow and dispersion of the reagents by the pressure-driven flow along the channel is large.

A significant amount of work has been done to solve the two problems of mixing and dispersion. For example, droplets have been used to eliminate dispersion in a complete DNA analyzer.[16] Droplets have been used in microchannnels before to perform chemical reactions and to enhance reactions that involve immiscible reagents.[17] Alternatively, mixing and transport of minute volumes of reagents without dispersion can be achieved by using fused vesicles.[18] Hydrodynamic focusing[19] is the most attractive microfluidic method for studies of macromolecular folding using small volumes of samples. It has demonstrated the value of microfluidics to biophysical measurements. This method solves the mixing problem by rapid injection of a stream containing the biomolecules between two flowing streams of excess of a folding buffer. The streams of buffer squeeze ("focus") the central stream to a thickness as low as ~100 nm, and mixing by diffusion occurs rapidly (less than 10 μs has been obtained[19]) as molecules diffuse in and out of the thin central stream. This method has been used to study folding on time scales of 150−500 μs,[20] −0.8 to 8.0 ms,[21] and 5−45 ms.[22] This droplet-based microfluidic system is complementary to hydrodynamic focusing. Mixing in this system is substantially slower than in hydrodynamic focusing, and due to the presence of liquid−liquid interfaces, the scattering measurements commonly used with hydrodynamic focusing may be more difficult to perform. On the other hand, in hydrodynamic focusing, one of the solutions of reagents must be used in excess, making it less attractive for those kinetic measurements (e.g., second-order) where concentrations of the reagents have to be controlled and varied. Varying concentrations is unnecessary for folding experiments.

(i) Rapid On-Chip Dilution. Typically, rate constants are obtained by performing kinetic measurements repeatedly under varying concentrations. Preparing solutions of various concentrations manually and performing an experiment at each of these concentrations is tedious and may require undesirably high volumes of samples. Microfluidic channels can be fabricated on a small scale with ease, and usually the microfluidic measurement itself does not require a large amount of sample. Most of the sample solution is often used to fill the inlets and outlets of the microfluidic device to interface it with the macroscopic world. When minimizing sample consumption is critical, the microfluidic system must be able to perform on-chip dilution[14,15,23] to perform measurements over a range of concentrations using only one set of stock solutions to fill the inlets. Such a system would also eliminate the need for manual dilutions.

Here, we describe how a series of reagent concentrations can be accessed quickly without disconnecting the inlet needles (Figure 1). Figure 2 shows formation of plugs from two streams of reagent solutions separated by a stream of buffer solution. In previous work,[1] the middle buffer stream was used to prevent the reagents from coming into contact prior to the formation of plugs. Here, the buffer stream performed an additional function: it was also used to control concentrations inside plugs by performing on-chip dilution. The concentrations inside the plug were controlled by varying the relative flow rates of the three

(6) Chan, C. K.; Hu, Y.; Takahashi, S.; Rousseau, D. L.; Eaton, W. A.; Hofrichter, J. *Proc. Natl. Acad. Sci. U.S.A.* **1997**, *94*, 1779−1784.
(7) Fang, X. W.; Thiyagarajan, P.; Sosnick, T. R.; Pan, T. *Proc. Natl. Acad. Sci. U.S.A.* **2002**, *99*, 8518−8523.
(8) (a) Ali, J. A.; Lohman, T. M. *Science* **1997**, *275*, 377−380. (b) Luo, L. S.; Burkart, M. D.; Stachelhaus, T.; Walsh, C. T. *J. Am. Chem. Soc.* **2001**, *123*, 11208−11218.
(9) (a) Brazeau, B. J.; Austin, R. N.; Tarr, C.; Groves, J. T.; Lipscomb, J. D. *J. Am. Chem. Soc.* **2001**, *123*, 11831−11837. (b) Valentine, A. M.; Stahl, S. S.; Lippard, S. J. *J. Am. Chem. Soc.* **1999**, *121*, 3876−3887.
(10) (a) Krantz, B. A.; Sosnick, T. R. *Biochemistry* **2000**, *39*, 11696−11701. (b) Halonen, P.; Baykov, A. A.; Goldman, A.; Lahti, R.; Cooperman, B. S. *Biochemistry* **2002**, *41*, 12025−12031.
(11) (a) Nelsen, S. F.; Ramm, M. T.; Ismagilov, R. F.; Nagy, M. A.; Trieber, D. A.; Powell, D. R.; Chen, X.; Gengler, J. J.; Qu, Q. L.; Brandt, J. L.; Pladziewicz, J. R. *J. Am. Chem. Soc.* **1997**, *119*, 5900−5907. (b) Cherry, J. P. F.; Johnson, A. R.; Baraldo, L. M.; Tsai, Y. C.; Cummins, C. C.; Kryatov, S. V.; Rybak-Akimova, E. V.; Capps, K. B.; Hoff, C. D.; Haar, C. M.; Nolan, S. P. *J. Am. Chem. Soc.* **2001**, *123*, 7271−7286.
(12) (a) Pandey, A.; Mann, M. *Nature* **2000**, *405*, 837−846. (b) Yarmush, M. L.; Jayaraman, A. *Annu. Rev. Biomed. Eng.* **2002**, *4*, 349−373.
(13) Kakuta, M.; Jayawickrama, D. A.; Wolters, A. M.; Manz, A.; Sweedler, J. V. *Anal. Chem.* **2003**, *75*, 956−960.
(14) Mao, H. B.; Yang, T. L.; Cremer, P. S. *Anal. Chem.* **2002**, *74*, 379−385.
(15) Kerby, M.; Chien, R. L. *Electrophoresis* **2001**, *22*, 3916−3923.
(16) Burns, M. A.; Johnson, B. N.; Brahmasandra, S. N.; Handique, K.; Webster, J. R.; Krishnan, M.; Sammarco, T.; Man, P. M.; Jones, D.; Heldsinger, D.; Mastrangelo, C. H.; Burke, D. T. *Science* **1998**, *282*, 484−487.
(17) (a) Burns, J. R.; Ramshaw, C. *Chem. Eng. Res. Des.* **1999**, *77*, 206−211. (b) Burns, J. R.; Ramshaw, C. *Chem. Eng. Commun.* **2002**, *189*, 1611−1628. (c) Harries, N.; Burns, J. R.; Barrow, D. A.; Ramshaw, C. *Int. J. Heat Mass Transfer* **2003**, *46*, 3313−3322.
(18) Chiu, D. T.; Wilson, C. F.; Ryttsen, F.; Stromberg, A.; Farre, C.; Karlsson, A.; Nordholm, S.; Gaggar, A.; Modi, B. P.; Moscho, A.; Garza-Lopez, R. A.; Orwar, O.; Zare, R. N. *Science* **1999**, *283*, 1892−1895.
(19) Knight, J. B.; Vishwanath, A.; Brody, J. P.; Austin, R. H. *Phys. Rev. Lett.* **1998**, *80*, 3863−3866.
(20) Pollack, L.; Tate, M. W.; Darnton, N. C.; Knight, J. B.; Gruner, S. M.; Eaton, W. A.; Austin, R. H. *Proc. Natl. Acad. Sci. U.S.A.* **1999**, *96*, 10115−10117.
(21) Pollack, L.; Tate, M. W.; Finnefrock, A. C.; Kalidas, C.; Trotter, S.; Darnton, N. C.; Lurio, L.; Austin, R. H.; Batt, C. A.; Gruner, S. M.; Mochrie, S. G. J. *Phys. Rev. Lett.* **2001**, *86*, 4962−4965.
(22) Russell, R.; Millettt, I. S.; Tate, M. W.; Kwok, L. W.; Nakatani, B.; Gruner, S. M.; Mochrie, S. G. J.; Pande, V.; Doniach, S.; Herschlag, D.; Pollack, L. *Proc. Natl. Acad. Sci. U.S.A.* **2002**, *99*, 4266−4271.
(23) Jiang, X. Y.; Ng, J. M. K.; Stroock, A. D.; Dertinger, S. K. W.; Whitesides, G. M. *J. Am. Chem. Soc.* **2003**, *125*, 5294−5295.

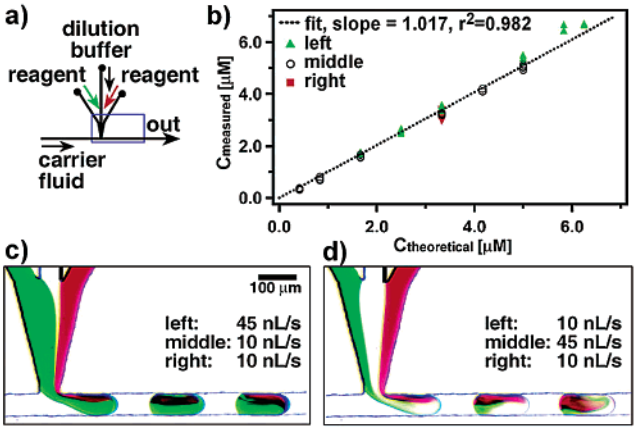

Figure 2. On-chip dilution was accomplished by varying the flow rates of the reagents. (a) A schematic of the microfluidic network. The blue rectangle outlines the field of view for images shown in parts c and d. (b) A graph quantifying this dilution method by measuring fluorescence of a solution of fluorescein diluted in plugs in the microchannel. Data are shown for 80 experiments in which fluorescein was flowed through one of the three inlets, where $C_{measured}$ and $C_{theoretical}$ [μM] are measured and expected fluorescein concentration. (c) and (d) Microphotographs illustrating this dilution method with streams of food dyes. Carrier fluid was flowed at 60 nL/s.

streams of stock solutions (Figure 2c,d). To ensure formation of plugs of identical size, the total flow rate of the three streams was kept constant. To validate this method of dilution, a solution of fluorescein was used as the quantitative fluorescent marker. We found that on-chip dilution of fluorescein was reliable (Figure 2b) when the flow rate of the fluorescein stream was varied between 4 and 63 nL/s. Thus, this approach enables kinetic measurements at varying concentrations without labor-intensive dilutions while minimizing sample consumption.

(ii) Accessing Multiple Time Ranges for Kinetics. Here, we show how this droplet-based microfluidic system can be used for measuring kinetics on both long and short time scales. In this system, the time scales accessed may be increased or decreased by varying the flow velocity accordingly. In addition, here we show that it has two attractive attributes. First, data can be acquired for a set of time points t_n separated by arbitrary intervals of time Δt_n. Second, kinetic data at all time points of that set can be acquired simultaneously.

Throughout this paper, we measured the kinetic activity of ribonuclease A (RNase A), a well-studied enzyme,[24] to demonstrate different features of this system. The kinetic measurements were performed by monitoring the steady-state fluorescence arising from the cleavage of a fluorogenic substrate[25] by RNase A[26] as the reaction mixture flowed down the channel. The amount of the product at a given time point t [s] was calculated from the intensity of fluorescence at the corresponding distance point d [m]. Because of the absence of dispersion, reaction time can be calculated at any distance, $t = d/U$ where U [m/s] is the velocity of the flow. For the microchannel designs used in this work, the winding section of the channel[1] was conserved to induce rapid mixing. After the winding section, the lengths of the straight channel can be designed to suit a particular time range.

(24) Raines, R. T. *Chem. Rev.* **1998**, *98*, 1045−1065.
(25) Kelemen, B. R.; Klink, T. A.; Behlke, M. A.; Eubanks, S. R.; Leland, P. A.; Raines, R. T. *Nucleic Acids Res.* **1999**, *27*, 3696−3701.
(26) The steady-state kinetic parameters for this enzyme and substrate were $k_{cat}/K_M = 43 \pm 1\ \mu M^{-1}\ s^{-1}$, $k_{cat} = 60 \pm 20\ s^{-1}$, and $K_M = 1.4 \pm 0.5\ \mu M$.

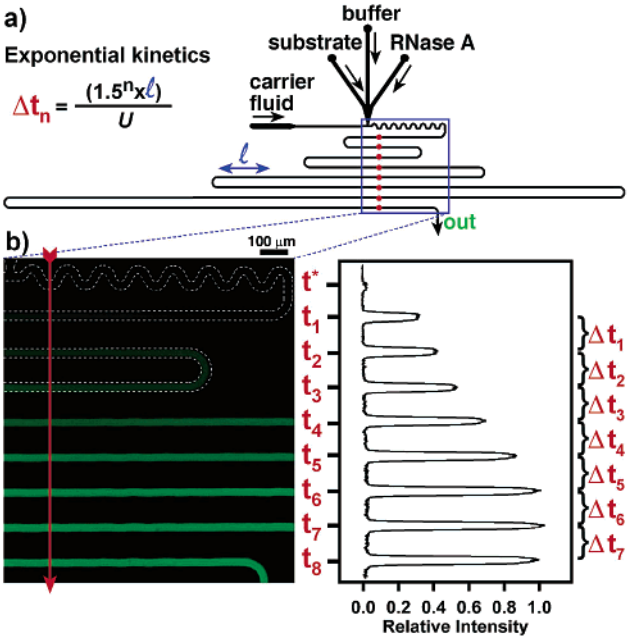

Figure 3. Figure 3. Design of microchannels for exponential kinetics. (a) A schematic of the microfluidic network. The blue rectangle outlines the field of view for the image shown in part b and ● indicates time points, t_n [s]. The time interval Δt_n was defined as shown. Within the field of view, kinetic data were obtained at t_n for a unit length l [m] and flow velocity U [m/s]. (b) Left: a false-color fluorescence microphotograph (4 s exposure; sample consumption was 33 nL/s) within the field of view. The dashed white lines trace the walls of the microchannel. Right: an intensity profile across the region of the microphotograph indicated by the red arrow. Left axis shows time points t_n, and right axis shows time intervals Δt_n.

Microchannels used in this droplet-based microfluidic system can be designed for any kinetic profile to accommodate the desired density of time points separated by arbitrary time intervals Δt_n. This capability is important because, in kinetics, not all time points are created equal. For most kinetic experiments, many time points are necessary in the beginning and fewer time points toward the end of the reaction. In first-order kinetics, time points should be separated exponentially. A set of time points separated by time intervals Δt_n can be achieved by combining the distance-time relationship ($t = d/U$) with rational design of microchannels. A set of time points with exponentially increasing time intervals Δt_n between the time points can be accessed by using exponentially increasing distances Δd_n [m]:

$$\Delta t_n = (\Delta d_n)/U = (m^n \times l)/U \qquad (1)$$

where m is the factor of exponential increase, n is the index (from 1 to z) numbering the time points, and l [m] is the unit length (Figure 3a). The z factor was determined by the number of rows of microchannel within the field of view ($z = 8$ in Figure 3). We also included a short segment of the winding channel that is necessary for rapid mixing by chaotic advection.[1] In Figure 3a, the time point t^* was within the winding channel, where mixing was not complete. For slower kinetics, U may be decreased and l may be increased to access a larger time range. Increasing m would give the most dramatic increase of the time range. For the design in Figure 3, the factors were defined to be $m = 1.5$, $l = 0.9$ mm, and $U = 106$ mm/s, giving an overall time range of ~450 ms.

Kinetic data within a set of time points can be acquired in parallel with this microfluidic platform. Continuous data col-

lection is not always attractive, especially for longer reactions with problems of photobleaching. For parallel data acquisition, all d_n were placed within the field of view of the microscope (Figure 3a). Within the acquired spatially resolved fluorescent image[3] (Figure 3b, left), only the detection area was exposed to minimize photobleaching. Each fluorescent image contained kinetic data at the desired density of time points to build a reaction progress curve. Using intensity profiles (as in Figure 3b, right), we used this exponential design to obtain kinetic measurements to establish compatibility with RNase A.

(iii) Biocompatibility. In this section, we describe a procedure that may be used to establish compatibility of this droplet-based microfluidic system with an enzyme, and we apply this procedure to RNase A. Biocompatibility of a microfluidic platform is necessary to ensure correct analysis of biological samples. In particular, we wished to address possible effects of the interface between the plug and the fluorinated carrier fluid. For vesicle systems involving interfaces with high surface-to-volume ratios, the interaction between the interface and the contained reactants is not trivial. In the limit of vesicles with diameters on nanometer scale, simulations suggested that kinetics are dictated by collisions between the reactants with the interface rather than each other.[27] This may be less of a problem in this system, where plugs have diameters on the order of tens of micrometers. However, at the hydrophobic interface between the plug and the carrier fluid, enzymes could denature and be rendered inactive.

The Selwyn's test[28,29] was successfully performed in this system to establish that there are no factors leading to RNase A denaturation or product inhibition. For a typical enzymatic reaction, the Michaelis−Menten equation[28] has the form

$$\frac{d}{dt}[P] = (V_m([S]_0 - [P]))/(K_M + [S]_0 - [P]) \qquad (2)$$

where $[S]_0$ is the initial substrate concentration, $[P]$ is the product concentration, V_m [M s^{-1}] is the maximum velocity, and K_M [M] is the Michaelis constant. Equation 2 can be integrated and rearranged:

$$[E]_0 \times t = (1/k_{cat}) \times ([P] - (K_M \times \ln(1 - ([P]/[S]_0)))) \quad (3)$$

where k_{cat} [s^{-1}] is the turnover number, $[E]_0$ is the initial enzyme concentration, and V_m can be defined as $(k_{cat} \times [E]_0)$. Equation 3 predicts that if the enzymatic reaction obeys the Michaelis−Menten equation and if there is no denaturation of the enzyme and no product inhibition, then plots of the time-dependent product formation $[P(t)]$ versus $([E]_0 \times t)$ at constant $[S]_0$ should result in superimposable curves for different $[E]_0$. A set of such plots is referred to as Selwyn's test.

To apply this test, both aspects of exponential design and on-chip dilution were used to obtain reaction progress curves for three RNase A concentrations at three substrate concentrations (5.0, 4.2, and 3.3 μM; in Figure 4, only the test for 3.3 μM is shown). We felt it was important to perform this test for several concentrations of substrate to exclude the possibility of coincidental overlap. From fluorescent images (as in Figure 3b), measurements were made for the time-dependent product formation $[P(t)]$ for three initial enzyme concentrations $[E]_0$ at three substrate concentrations each (Figure 4a). Then, data were plotted for $[P(t)]$ versus $([E]_0 \times t)$, which gave superimposable curves (Figure 4b). This test was successful for all three substrate concentrations. Therefore, this droplet-based microfluidic system proved to be compatible with this particular enzyme, although more work will be required to establish compatibility of this platform with other enzymes. This result may not be so surprising, given that RNase A is a fairly stable enzyme and that the aqueous solutions are inside of plugs that are completely surrounded by the fluorocarbon fluid and do not come in contact with the walls of the device. Fluorocarbon fluids are biocompatible, and previous works have used fluorocarbon fluids for blood transfusions[30] and liquid ventilation of fetuses,[31] both in humans.

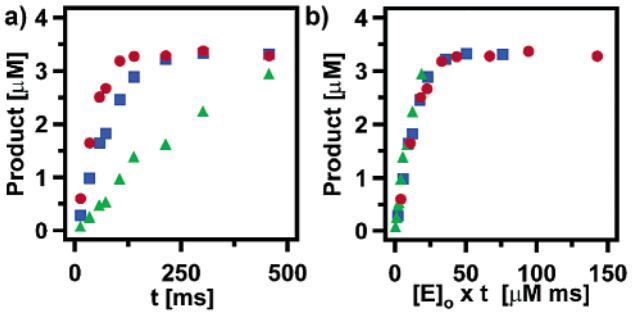

Figure 4. Measuring exponential kinetics of RNase A and Selwyn's test. (a) Graph of experimental data (obtained from images such as that shown in Figure 3b) for 3.3 μM substrate at three RNase A concentrations (● 0.3 μM, ■ 0.2 μM, ▲ 0.04 μM). (b) Graph of Selwyn's test from experimental data in part a. Superimposable plots show absence of RNase A denaturation or product inhibition.

(iv) Explicitly Accounting for the Effect of Mixing. We propose and validate a method of performing high-resolution kinetic measurements in microfluidic channels. This method treats mixing explicitly and consists of three steps: (i) quantifying mixing by measuring the mixing function $f_M(t)$ of the microfluidic system used for kinetic measurements, (ii) measuring reaction kinetics, and (iii) extracting kinetic parameters at high-resolution from kinetic data using a mathematical model that relies on $f_M(t)$ to take mixing into account.

For slow kinetic measurements, where the mixing time is only a small fraction of the overall reaction time, explicit treatment of mixing is not necessary. This was the case in the exponential measurements we performed to establish biocompatibility (Figure 3). For rapid kinetic measurements, mixing time is the limiting factor that determines the resolution. Mixing is rapid but difficult to quantify when using stopped-flow instruments; because of "dead time" the reaction mixture cannot be observed from $t = 0$ to $t \approx 1$ ms of the reaction and mixing time. An attractive feature of this droplet-based microfluidic system is that the reaction mixture can be observed at $t = 0$ (there is no dead time). In previous work, we took advantage of this feature and demonstrated that mixing could be quantified by measuring the rate of a diffusion-controlled Fluo-4/Ca^{2+} binding reaction.[1]

(27) Wilson, C. F.; Chiu, D. T.; Zare, R. N.; Stromberg, A.; Karlsson, A.; Orwar, O. Confining and Probing Single Molecules in Synthetic Liposomes. In *Single Molecule Spectroscopy: Nobel Symposium Lectures*; Rigler, R., Orrit, M., Basche, T. (Eds.); Springer-Verlag: Berlin, 2001; pp 130−143.
(28) Duggleby, R. G. In *Enzyme Kinetics and Mechanism, Pt D*; Academic Press: San Diego, 1995; Vol. 249, pp 61−90.
(29) Selwyn, M. J. *Biochim. Biophys. Acta* **1965**, *105*, 193−195.
(30) Squires, J. E. *Science* **2002**, *295*, 1002.
(31) Leach, C. L.; Greenspan, J. S.; Rubenstein, S. D.; Shaffer, T. H.; Wolfson, M. R.; Jackson, J. C.; DeLemos, R.; Fuhrman, B. P. *N. Engl. J. Med.* **1996**, *335*, 761−767.

This approach relies on the conversion between space and time performed by the fluid flow, $t = d/U$. There are two different time resolutions that we consider here: time resolution with which the measurement can be performed and the time resolution with which kinetic information can be extracted. The limit of time resolution of the measurement equals lp/U, where lp is the length of plugs [m]. In this work, $lp \approx 40\ \mu$m and $U \approx 400$ mm/s; therefore, the resolution of the measurements itself is approximately equal to 100 μs. The time resolution with which kinetic information can be extracted is limited by the mixing time (~1.5 ms). In this droplet-based microfluidic system system, the time resolution of the measurement is high enough so that the mixing function can be determined accurately. Then, the mixing function can be incorporated into the kinetic model so the kinetic parameters can be extracted with resolution not limited by mixing. We used the Fluo-4/Ca^{2+} binding reaction[1] (Figure 5b,c; open symbols) and corrected for diffusion coefficients[32] to determine $f_M(t)$, the mixing function that describes the fraction of solution mixed as a function of time (Figure 5b,c; dashed lines). For chaotic mixing, the mixing function $f_M(t)$ has sigmoidal shape, where $f_M(0) = 0$ at $t = 0$ and $f_M(t) = 1$ at t when mixing is complete.

Mixing is easy to incorporate explicitly into a kinetic model. Consider a kinetic model $F(k, [S])$ that describes the concentration of product $[P]$ as a function of time t, the rate constant k, and first-order substrate concentration $[S]$:

$$[P(t)] = F(k, [S], t) \tag{4}$$

Slow mixing delays the beginning of the reaction. During the time interval $\Delta\tau_i = \tau_{i+1} - \tau_i$, a small fraction of the reaction mixture $\Delta f_M(\tau_i) = f_M(\tau_{i+1}) - f_M(\tau_i)$ mixes and begins reacting with the time delay of τ_i. Overall, the whole reaction may be described as:

$$[P(t)] = \sum_i \Delta f_M(\tau_i) F(k,[S],t - \tau_i) \tag{5}$$

This equation may be converted to an equivalent integral-differential form for convenience:

$$[P(t)] = \int_0^\infty f'_M(\tau) F(k,[S],t - \tau)\, d\tau \tag{6}$$

where $f'_M(\tau)$ is the derivative of the mixing function and τ is the integration time variable.

This treatment is justified for a model described by eq 4, but will not be correct for complex kinetic models, especially those involving autocatalytic reactions.[33]

Millisecond Single-Turnover Kinetics. In this section, we discuss measuring millisecond single-turnover kinetics of RNase A by using nanoliters of solutions. This experiment used all of the new features of the droplet-based microfluidic system: on-chip dilution, proper microchannel design, compatibility with the enzyme, and explicit treatment of mixing.

Single-turnover kinetics require high concentrations of both the enzyme and the substrate, with the enzyme used in large excess.[34] Therefore, mixing must be rapid and sample consumption must be low. For most microfluidic systems, sample consumption is low but mixing is often too slow. For stopped-flow, mixing is rapid but sample consumption is high. Submicroliter sample consumption and rapid mixing makes this droplet-based microfluidic system especially attractive for performing such measurements.

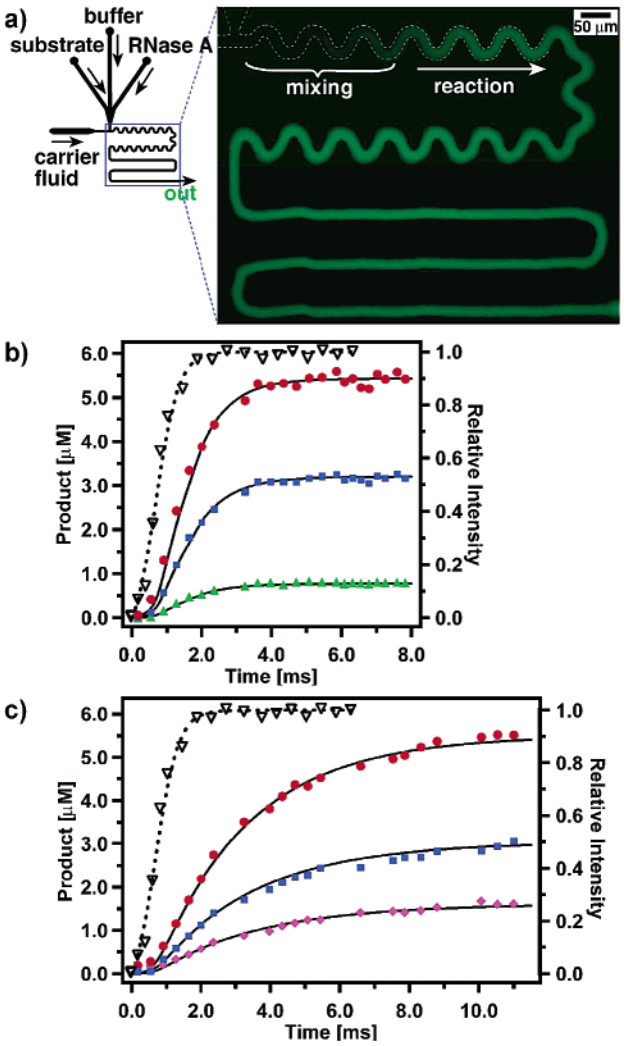

Figure 5. Measuring single-turnover kinetics of RNase A. (a) Left: a schematic of the microfluidic network. Right: a false-color fluorescence microphotograph (2 s exposure showing time-averaged fluorescence intensity of moving plugs and oil; sample consumption was 33 nL/s). The dashed white lines trace the walls of the microchannel. (b) Graph of reaction progress at a pH of 7.5. Shown are experimental kinetic data (left axis) for three substrate concentrations (● 5.8 μM, ■ 3.3 μM, ▲ 0.8 μM) obtained from images such as that shown in part a with fits of the reaction progress (solid lines). Also shown is a mixing curve using the Fluo-4/Ca^{2+} system (right axis, ▽ in the same microfluidic device with fit (dashed line) of an explicit mixing function). (c) Graph of reaction progress at pH of 6.0. Shown are experimental kinetic data (left axis) for three substrate concentrations (● 5.8 μM, ■ 3.3 μM, ◆ 1.6 μM) with fits of the reaction progress (solid lines). Also shown is the same mixing curve as in part b.

We performed the measurement in the device shown in Figure 5a. We designed the device to obtain a continuous kinetic profile and used on-chip dilution to control concentrations during the experiment. In a single experiment, we obtained eight progress curves (only three are shown, Figure 5b) at eight concentrations of the substrate to ensure that the measurement is in the single-

(32) Song, H.; Bringer, M. R.; Tice, J. D.; Gerdts, C. J.; Ismagilov, R. F. *Appl. Phys. Lett.* **2003**, in press.
(33) (a) Metcalfe, G.; Ottino, J. M. *Phys. Rev. Lett.* **1994**, *72*, 2875−2878. (b) Zumofen, G.; Klafter, J.; Shlesinger, M. F. *Phys. Rev. Lett.* **1996**, *77*, 2830−2833.
(34) Fierke, C. A.; Hammes, G. G. In *Enzyme Kinetics and Mechanism, Pt D*; Academic Press: San Diego, 1995; Vol. 249, pp 3−37.

turnover regime. In addition, each progress curve at each concentration was obtained two to three times to ensure reproducibility.

For single-turnover kinetics, $[E]_0 \gg [S]_0$ and the simple reaction equation is:

$$[P(t)] = [S]_0(1 - \exp(-kt)) \quad (7)$$

where k [s^{-1}] is the single-turnover rate constant. The reaction under study is known to occur on a single-millisecond time scale. Mixing also occurs on this time scale. Therefore, explicit treatment of mixing is clearly necessary in this case to extract accurate kinetic information from kinetic measurements.

To account for mixing, we obtained the mixing function $f_M(t)$ (plotted as dashed lines in Figure 5b,c) from Fluo-4/Ca^{2+} data (plotted as open symbols in Figure 5b,c) for the microfluidic device used and then performed two fits to the kinetic data of RNase A. The first fit was obtained with eq 8, which used the discretized form of $f_M(t)$ in the spirit of eq 5. This fit accounted for the time delay τ required to mix a fraction of the reaction mixture $\Delta f_M(t)$:

$$[P(t)] = [S]_0 \sum_i \Delta f_M(\tau_i)(1 - \exp(-k(t - \tau_i))) \quad (8)$$

We found it more convenient to work with the integral-differential eq 9, analogous to eq 6:

$$[P(t)] = [S]_0 \int_0^\infty f'_M(\tau)(1 - \exp(-k(t - \tau)))\, d\tau \quad (9)$$

The two equations produced indistinguishable fits (only fits to eq 9 are shown in Figure 5b,c). All eight progress curves gave an excellent fit to the same rate constant of 1100 ± 250 s^{-1} (Figure 5b, only three are shown). These results are in agreement with previous studies, where cleavage rate constants of oligonucleotides by ribonucleases were shown to be $\sim 10^3$ s^{-1}.[35]

Mixing function is an intrinsic property of each microfluidic device in this droplet-based microfluidic system and has to be measured only once. Enzymatic activity of RNase A is pH-dependent, with the cleavage step being optimal at a pH of ~7.5. To confirm that the same mixing function may be used for different kinetic experiments, the single-turnover reaction was performed at a lower pH of 6.0. The data were fit to eq 9 using the same mixing function. At a pH of 6.0, the rate constant obtained from the fits decreased 3-fold to 350 ± 50 s^{-1} (Figure 5c), in full agreement with previous studies.[36]

Conclusions

In conclusion, kinetic measurements can be performed rapidly and economically using this droplet-based microfluidic system, and kinetic information can be extracted with better than millisecond resolution. Concentrations within the plugs may be controlled easily by on-chip dilution. On-chip control of concentrations is especially important for kinetic measurements and will minimize sample consumption and manual labor. This feature should be also important for performing quantitative assays on a chip. In this work, each kinetic profile was acquired in a single fluorescence image in 2−4 s and required less than 75−150 nL of the reagent solutions. The 2 μL volumes shown in Figure 1 are sufficient for ~15 kinetic experiments over a range of concentrations. These experiments with stopped-flow would have required at least several hundreds of microliters of solutions.[10] Channels may be designed for efficient measurements of arbitrary kinetic profiles by obtaining virtually any sequence of time points from a single image. This approach is applicable to most systems that operate in a continuous flow mode and that use spatially resolved imaging to obtain time-resolved information. We used this approach together with varying concentrations to demonstrate how biocompatibility for an enzyme may be established reliably in a single experiment. It would be straightforward to use this approach to establish compatibility (or the lack of compatibility) of this droplet-based microfluidic system with other enzymes; such work would be important if this system is to be used for assays involving enzymes and other biomolecules.

In the absence of additional mathematical treatment, the time resolution of this platform for extracting kinetic parameters from measurements would be limited by the mixing time (~1.5 ms), rather than the resolution of the measurement itself (~100 μs). As described in our previous work,[1] there is no dead time in this system, and mixing may be carefully quantified. Here, we described and implemented a mathematical treatment of reaction kinetics together with mixing to improve the time resolution with which kinetic parameters are extracted. This method would be valuable in other systems where mixing can be measured with high resolution[2] and described in the form of a mixing function. Using this method, we were able to extract a single turnover rate constant for RNase A with better than millisecond resolution. Currently, detection in this droplet-based microfluidic system is limited to optical methods and requires labeling of reagents with fluorophores or chromophores, and more development would be required to overcome this limitation. However, for systems where fluorescence may be used for detection, this system may serve as an inexpensive and economical complement to stopped-flow methods for a broad range of kinetic experiments and assays in chemistry and biochemistry.

Experimental Section

I. Materials. Poly(dimethylsiloxane) (PDMS, Sylgard Brand 184 Silicone Elastomer Kit) was obtained from Dow Corning. Tris(hydroxymethyl)aminomethane (Tris base), disodium ethylenediamine tetraacetic acid (EDTA, free acid), 1-(*N*-morpholino)ethanesulfonic acid (MES), 3-(*N*-morpholino)propanesulfonic acid (MOPS), phosphate-buffered saline (PBS, 10×), fluorescein (disodium salt), and glass coverslips (Premium Coverslips, #1) were obtained from Fisher Scientific. (Tridecafluoro-1,1,2,2,-tetrahydrooctyl)-1-trichlorosilane was obtained from United Chemical Technologies, Inc. Perfluorohexane (95%) and 1*H*,1*H*,2*H*,2*H*-perfluoro-1-octanol (98%) were obtained from Alfa Aesar. Perfluoro(1,3-dimethylcyclohexane) (80%) was obtained from Aldrich. The colored dyes were McCormick red food coloring (water, propylene glycol, FD&C reds 40 and 3, propylparaben) and McCormick green food coloring (water, propylene glycol, FD&C yellow 5, FD&C blue 1, propylparaben). Fluo-4 (pentapotassium salt) was obtained from Molecular Probes, Inc. Calcium chloride dihydrate (+99%) was obtained from Aldrich. Ribonuclease A solution (EC 3.1.27.5) was obtained from USB Corp. and generously provided by A. V. Korennykh and Prof. J. A. Piccirilli. The RNaseAlert QC System was obtained from Ambion Inc., which included the RNaseAlert substrate and RNase*Zap* decontaminant solution.

II. Fabrication of Devices. Microchannels were fabricated with rectangular cross-sections using rapid prototyping in PDMS.[5] PDMS/

(35) Thompson, J. E.; Raines, R. T. *J. Am. Chem. Soc.* **1994**, *116*, 5467−5468.
(36) Witzel, H. *Prog. Nucleic Acid Res.* **1963**, *2*, 221−258.

PDMS devices and PDMS/glass devices were sealed using a PDC-001 Plasma Cleaner from Harrick Scientific Corporation. For PDMS/PDMS devices, microchannels were rendered hydrophobic by baking in a 120 °C oven for at least 1 h. For PDMS/glass devices, microchannels were rendered hydrophobic by using dry N_2 at 70 mmHg to flow (tridecafluoro-1,1,2,2,-tetrahydrooctyl)-1-trichlorosilane vapor through the device for 30 min.

III. Microfluidic Experiments. Syringe pumps were used to drive flows (Harvard Apparatus PHD 2000 Infusion pumps). For aqueous solutions, 50-μL Hamilton Gastight syringes (1700 series, RN) with removeable needles of 27 gauge were used with 30-gauge Teflon tubing from Weico Wire & Cable. For the carrier fluid, 1-mL Hamilton Gastight syringes (1700 series, TLL) were used with 30-gauge Teflon needles with one hub from Hamilton.

Optical microphotographs were acquired with a Leica MZ12.5 stereomicroscope with a SPOT Insight color digital camera (model #3.2.0, Diagnostic Instruments, Inc.). The program used to collect images was SPOT Advanced software (version 3.4.0 for Windows) from Diagnostic Instruments. Lighting was provided by a Machine Vision Strobe X-Strobe $\times$1200 (20 Hz, 12 μF, 600 V) from Perkin-Elmer Optoelectronics. To obtain an image, the shutter of the camera was opened for 1 s and the strobe light was lit for approximately 10 μs. Fluorescence microphotographs were acquired using a Zeiss Axioplan microscope with a CoolSNAP fxHQ digital camera (12-bit, 1392 $\times$ 1040 resolution) from Roper Scientific. The program used to collect images was OPENLAB from Improvision, Ltd. Lighting was provided by a Hg light source. Images were integrated for 2−4 s; the resulting fluorescence microphotograph showed the average fluorescence intensity of constantly moving plugs of reagents and carrier fluid. The photobleaching was minimized because each plug containing reagents was exposed for no longer than the plug's residence time within the field of view of the microscope. For example, at a flow velocity of 200 mm/s and the length of the channel within the field of view of ~10 mm the exposure was limited to 0.05 s.

IV. Analyzing Fluorescence Images. Images were analyzed using Image J from NIH Image software. A region of interest (ROI) was selected at a specific height and width. This ROI was used to obtain an intensity profile across the width of the microchannel (as in Figure 3b, right). Intensity profiles were acquired at a particular microchannel distance from the plug-forming junction. The area between the curve and the background baseline was considered to be the integrated intensity at that channel distance d_n. This channel distance was converted into reaction time t_n by dividing it by the velocity of the flow U [m/s], obtained from the known volumetric flow rate and cross-section of the microchannel.

To compensate for spatial nonuniformity of the illumination of the Hg light source, a solution of fluorescein was used as the stock solution to form plugs of fluorescein and fluorescent images were acquired in the same field of view. At each experimental d_n, fluorescein plug intensity profiles were obtained using the same ROI and integrated intensities were measured. The reaction intensity data were normalized by dividing the reaction intensities by the fluorescein plug intensities.

V. Quantifying On-Chip Dilution. For all experiments, the carrier fluid was a mixture of three fluorinated fluids: perfluorohexane, perfluoro(1,3-dimethylcyclohexane), and 1*H*,1*H*,2*H*,2*H*-perfluoro-1-octanol at a ratio of (8.5:1.5:1), respectively. To quantify on-chip dilution (Figure 2b), fluorescence of fluorescein was measured. One stream of the inlet contained 8 μM fluorescein; the other two inlets contained 1$\times$ PBS buffer. The flow rate of the right stream was always kept constant at 33 nL/s, while the flow rates of the middle and left streams were varied. The overall flow rate of the three inlets was kept at 100 nL/s. Fluorescence images were integrated for 2 s and analyzed as above. To visualize on-chip dilution (Figure 2c,d), the red streams were McCormick red food coloring, the green streams were McCormick green food coloring diluted 1:1 with water, and the dilution stream was water.

VI. Measuring Slower Kinetics and Selwyn's Test. In the exponential microchannel design (Figure 3b), the three stock solutions in the aqueous syringes were 10 μM RNaseAlert in TE buffer (10 mM Tris, 1 mM EDTA, pH = 7.5 titrated with 1 M HCl, T = 30 °C), TE buffer, and 0.5 μM RNase A in TE buffer. Prior to filling the syringes, RNase*Zap* was used to decontaminate surfaces. Microchannel dimensions were 50 μm wide and 50 μm high. Fluorescence images were integrated for 4 s and analyzed as above.

VII. Measuring Single-Turnover Kinetics. In the microchannel design of Figure 5, three different experiments were performed. First, mixing was quantified using the Fluo-4/Ca^{2+} system[1] (Figure 5b, mixing curve) and corrected for differences in diffusion constants.[32] The three stock solutions in the aqueous syringes were 55.7 μM Fluo-4 in MOPS (20 mM, pH = 7 titrated with 1 M HCl, faint background fluorescence of Fluo-4 was quenched with 6 μM EDTA, T = 30 °C), MOPS buffer, and 850 μM $CaCl_2$ in MOPS. Microchannel dimensions were 20 μm wide and 50 μm high. Fluorescence images were integrated for 2 s and analyzed as above. Second, single-turnover kinetics were performed at a pH of 7.5 (Figure 5b, left). The three stock solutions in the aqueous syringes were 10 μM RNaseAlert in TE buffer (10 mM Tris, 1 mM EDTA, pH = 7.5 titrated with 1 M HCl, T = 30 °C), TE buffer, and 146 μM RNase A in TE buffer. Fluorescence images were integrated for 2 s and analyzed as above. Third, single-turnover kinetics were performed at a pH of 6.0 (Figure 5b, right). The three stock solutions in the aqueous syringes were 10 μM RNaseAlert in MES buffer (50 mM, pH = 6.0 titrated with 1 M NaOH), MES buffer, and 146 μM RNase A in MES buffer. Fluorescence images were integrated for 4 s and analyzed as above.

VIII. Data Analysis. Using Microsoft Excel and Igor Pro, we fit the mixing data with a sigmoidal function[37] to obtain the mixing function $f_M(\tau)$. Sigmoidal functions are easily differentiated and integrated and are commonly used for modeling (e.g., responses of neurons,[38] which are similar to the shape of the mixing function). Using the mixing function with eqs 8 and 9, we determined kinetic parameters for the RNase A reaction as described in the text. For all rate constants, the reported error takes into account both the error of the fit and the experimental errors. This estimate of the error was made by analyzing several experiments performed on different days with different batches of solutions.

Acknowledgment. This work was supported by the NIH (R01 EB001903), the Beckman Young Investigator program, Searle Scholars Program, the Predoctoral Training Grant (H.S.) of the NIH (GM 08720), and the Camille and Henry Dreyfus New Faculty Award. At The University of Chicago, work was performed at the MRSEC microfluidic facility funded by the NSF and at the Cancer Center DLMF. Photolithography was performed at MAL of the UIC. We thank A.V. Korennykh and Prof. J. A. Piccirilli for helpful suggestions and for providing samples of RNase A, Prof. T. R. Sosnick and Prof. T. Pan for helpful discussions, and J.D. Tice for the image shown in Figure 1 and for invaluable experimental assistance.

JA0354566

(37) Råde, L.; Westergren, B. *Mathematics Handbook for Science and Engineering*, 4th ed.; Springer-Verlag: Berlin, 1999.
(38) Haykin, S. *Neural Networks*; Prentice Hall: Upper Saddle River, NJ, 1994.